DIGITAL SIGNAL PROCESSING 4, 127–140 (1994)

A Real-Time Signal Processing Technique for Approximating a Function by a Sum of Complex Exponentials Utilizing the Matrix-Pencil Approach

Tapan K. Sarkar,*,† Fengduo Hu,‡ Yingbo Hua,§ and Michael Wicks¶,**

*Department of Electrical and Computer Engineering, 121 Link Hall, Syracuse University, Syracuse, New York 13244-1240; ‡Zilog Incorporated, MSD2-3, 210 E. Hacienda Avenue, Campbell, California 95008; §Department of Electrical Engineering, University of Melbourne, Melbourne, Parkville, Victoria, Australia 3052; ¶Rome Laboratory, Directorate of Surveillance and Photonics, Griffiss Air Force Base, New York 13441

Sarkar, T. K., Hu, F., Hua, Y., and Wicks, M., A Real-Time Signal Processing Technique for Approximating a Function by a Sum of Complex Exponentials Utilizing the Matrix-Pencil Approach, *Digital Signal Processing* 4 (1994), 127–140.

In this paper, the development of the matrix-pencil technique is presented, including a historical overview and recent generalizations. It has been shown that this method is computationally efficient and robust to noise. A band-pass version of this approach has been implemented in hardware utilizing an AT&T DSP32C chip, to perform real-time target identification.

1. INTRODUCTION

The response of an object subjected to a burst of electromagnetic energy is of great interest for applications in numerous electronic systems. The development of the singularity expansion method (SEM) by Baum [1] provides a convenient method to describe the late time response of antennas (and other scatterers) by defining natural frequencies, modes (or poles) and coupling coefficients. In essence, this is equivalent to modeling the late time response of an object to an electromagnetic pulse by a sum of complex exponentials. The complex exponentials describe the modes, with amplitude related to coupling coefficient, indicating which modes are present. It has been shown for antennas of finite size, that the current induced on an object, and the radiated electromagnetic fields due to these induced currents, may be modeled by autoregressive moving average (ARMA) processes when there are no branch cuts in the complex plane [2]. Note that it has been numerically verified that all poles are simple for perfectly conducting bodies [3]. Since the complex frequencies comprising the electromagnetic response of an object is an intrinsic property of that object, the poles extracted from the late time response of the scattered fields may be utilized to provide a means for radar target identification [4,5].

In general, the model of the observed late time response can be formulated as

$$y(t) = x(t) + n(t) \approx \sum_{i=1}^{M} R_i \exp(s_i t) + n(t), \qquad 0 \leq t \leq T, \quad (1.1)$$

where

$y(t)$ = observed time response
$n(t)$ = noise in the system
$x(t)$ = signal
R_i = residues or complex amplitudes
$s_i = -\alpha_i + j\omega_i$
α_i = damping factors
ω_i = angular frequency ($\omega_i = 2\pi f_i$).

† Supported in part by Scientific-Atlanta.

** On LTFTS at Syracuse University.

1051-2004/94 $5.00

After sampling, the time variable t is replaced by kT_s, where T_s is the sampling period. The sequence can be rewritten as

$$y(kT_s) = x(kT_s) + n(kT_s) \approx \sum_{i=1}^{M} R_i z_i^k + n(kT_s)$$
$$\text{for} \quad k = 0, 1, \ldots, N-1, \quad (1.2)$$

where

$$z_i = e^{s_i T_s} = e^{(-\alpha_i + j\omega_i)T_s} \quad \text{for} \quad i = 1, 2, \ldots, M. \quad (1.3)$$

Now, the objective is to find the best estimates of M, R_i and z_i from noise-contaminated measurement data. In the most general case, this problem is essentially nonlinear; however, it is often linearized [6] for ease of solution.

A technique for approximating a function by a sum of complex exponentials is used by Marin and Latham [2], and was first developed by Prony [7] in 1795, then refined by Hilderband [8] in 1956 and VanBlaricum and Mittra [9] in 1975. This method is efficient and accurate for extracting poles (and residues) from equally spaced samples of transient phenomena. However, Prony's method is extremely sensitive to noise. To combat noise introduced into the measurement data, Prony's method maybe modified to incorporate techniques for systematically determining the number of poles using Householder's orthogonalization, as well as the dominant eigenvalue/eigenvector method [10]. This motivated Tufts and Kumaresan to propose an application of the principal eigenvector method based on a singular value decomposition (SVD) of the data matrix prior to applying Prony's method [11,12].

In this paper, it will be shown that estimates computed using the Matrix-Pencil (MP) method are not only more efficient than those computed using a Prony based technique, but also are statistically superior to the Tufts–Kumaresan method [18,27,30]. The MP Method is also a generalization of the pencil-of-functions method.

2. PENCIL-OF-FUNCTION METHOD

The term "pencil" originated with Gantmacher [13] in 1960. Similar to Gantmacher's definition for matrix pencil, another useful mathematical entity arises when combining two functions defined on a common interval with a scalar parameter λ,

$$f(t, \lambda) = g(t) + \lambda h(t); \quad (2.1)$$

$f(t, \lambda)$ is called a pencil-of-functions $g(t)$ and $h(t)$, parameterized by λ. To avoid obvious triviality, $g(t)$ is not permitted to be a scalar multiple of $h(t)$.

The pencil-of-functions will contain very important features when $g(t)$, $h(t)$, and λ are appropriately selected. But first, the pencil-of-function method is introduced from a historical perspective [14–17] initially used to approximate a function by a sum of complex exponentials.

Let the signal $y(t)$ (1.1) be processed by a series of cascaded filters. The family of signals $\{y_0(t), y_1(t), \ldots, y_m(t)\}$ are called information signals, and are defined as

$$y_0(t) = y(t)$$

and

$$y_i(t) = Q[y_{i-1}(t)], \quad (2.2)$$

where $Q[\cdot]$ denotes a filtering operation on the argument function. Here we assume $Q[\cdot]$ will filter noise while not significantly affecting the poles, s_i, of the signal defined in Eq. (1.1).

Since the functions $y_0(t), y_1(t), \ldots, y_M(t)$ span a common M-dimensional subspace spanned by $\exp(s_i t)$, $i = 1, \ldots, M$, the functions $y_0(t), y_1(t), \ldots, y_{M-1}(t)$ are linearly independent. While the functions $y_0(t), y_1(t), \ldots, y_{M-1}(t), y_M(t)$ are linearly dependent, the linear independence of the set of pencil-of-functions

$$\{y_{i-1}(t) - \lambda y_i(t)\} \quad (2.3)$$

for $i = 1, 2, \ldots, M$, depends on the choice of λ. The question is, for what values of the parameter λ does the pencil become linearly dependent, and how does λ relate to s_i. To address the first part of this question, the pencil defined by Eqs. (2.1)–(2.3) becomes linearly dependent when the determinant of the Gram matrix, $[F]$, is zero:

$$[F] = \begin{bmatrix} \langle y_0 - \lambda y_1; y_0 - \lambda y_1 \rangle & \cdots & \langle y_0 - \lambda y_1; y_{M-1} - \lambda y_M \rangle \\ \vdots & \ddots & \vdots \\ \langle y_{M-1} - \lambda y_M; y_0 - \lambda y_1 \rangle & \cdots & \langle y_{M-1} - \lambda y_M; y_{M-1} - \lambda y_M \rangle \end{bmatrix}. \quad (2.4)$$

The inner product is defined as

$$\langle c; d \rangle = \int_t c(t)\,\overline{d(t)}\,dt, \tag{2.5}$$

and the overbar denotes the complex conjugate.

The determinant of the gram matrix $[F]$ is then given by

$$\det[F] = \sum_{i=1}^{M+1} \sum_{j=1}^{M+1} \Delta_{ij} (-\lambda)^{M+1-i} (-\bar{\lambda})^{M+1-j}, \tag{2.6}$$

where Δ_{ij} is the (i, j)th minor of the matrix $[G]$ defined by

$$[G] = \begin{bmatrix} \langle y_0; y_0 \rangle & \langle y_0; y_1 \rangle & \cdots & \langle y_0; y_M \rangle \\ \langle y_1; y_0 \rangle & \langle y_1; y_1 \rangle & \cdots & \langle y_1; y_M \rangle \\ \vdots & \vdots & & \vdots \\ \langle y_M; y_0 \rangle & \langle y_M; y_1 \rangle & \cdots & \langle y_M; y_M \rangle \end{bmatrix}. \tag{2.7}$$

If $\det[F]$ is set equal to zero, one obtains

$$\sum_{i=1}^{M+1} \sqrt{\Delta_{ii}}\,\lambda^{M-i+1} = 0. \tag{2.8}$$

It is now shown that the poles s_i can be obtained from λ once the filters, Q, are specified. We consider three special cases [18,19].

(i) Q Specified as a Reverse Time Integration Filter

If Q is defined as the (reverse time) integral of the signals from ∞ to t, then

$$y_i(t) = \int_{\infty}^{t} y_{i-1}(\tau)\,d\tau \quad \text{for} \quad i = 1, \ldots, M, \tag{2.9}$$

and

$$y_i(t) \approx \sum_{j=1}^{M} \frac{R_j}{s_j^i} \exp(-s_i t), \quad i = 1, 2, \ldots, M.$$

Hence,

$$y_{i-1}(t) - \lambda y_i(t) \approx \sum_{j=1}^{M} \frac{R_j}{s_j^i} (s_j - \lambda) \exp(-s_j t), \quad i = 1, 2, \ldots, M. \tag{2.10}$$

It can be shown that the pencil-of-functions defined by (2.3) will be linearly dependent if λ is one of the system poles. Its value is obtained from the solution of Eq. (2.8) [20]. Estimates obtained through the solution of (2.10) are related to the best least-squares estimate of the pole, s_i^{BLS}, in the following manner [14–17]:

$$s_i = s_i^{\mathrm{BLS}} + \epsilon l_i + \mathrm{O}(\epsilon^2). \tag{2.11}$$

The l_i are unspecified constants, and ϵ is the integral squared error of the approximation to the function. Here $\mathrm{O}(\epsilon^2)$ implies the remainder is on the order of ϵ^2. It is interesting to note that the approximation to s_i is continuously differentiable with respect to ϵ. Hence as ϵ approaches zero, the suboptimal poles approach the best least squares poles in a continuous fashion. It also can be shown that

$$\sqrt{|G_{n+1}|} = \mathrm{O}(\epsilon). \tag{2.12}$$

The operator involved in this technique is the reverse time integral operator, which integrates a function from ∞ to t. For an exponential basis the operator maps the space onto itself while preserving the natural frequency of the exponentials. It is this property which makes the method robust to noise.

(ii) Q Specified as a Low-Pass Filter

In this case, IIR filters are used for the realization of Q. In general, the implementation of an IIR filter is a forward adaptive process, that is, the output of the filter, $y(k)$, is a linear combination of the past and present input signals $x(k)$, as well as past values of the output.

Specifically

$$y(k) = \sum_{j=0}^{m} b_j x(j-k) - \sum_{i=1}^{n} a_i y(i-k), \tag{2.13}$$

which yields

$$Y(z) = X(z) \cdot H(z), \tag{2.14}$$

where

$$H(z) = \frac{b_0 + b_1 z^{-1} + \cdots + b_m z^{-m}}{1 + a_1 z^{-1} + \cdots + a_n z^{-n}}. \tag{2.15}$$

It is apparent that the output of this filter contains both the poles of the input signal and those of the filter. If the input signal is assumed to be a linear combination of exponentially damped sinusoidal signals, we can utilize a backward recursive process to force the filtered data to contain only the poles of the desired signal. The backward process enables one to separate the poles of the signal from the poles of the filter (which are located outside the unit circle). The backward recurrence can be written as

$$y(k) = \sum_{j=0}^{m} b_j x(j+k) - \sum_{i=1}^{n} a_i y(i+k), \quad (2.16)$$

and the poles of the filter are the roots of

$$\sum_{i=0}^{n} a_i z^i = 0 \quad \text{with} \quad a_0 = 1. \quad (2.17)$$

If the poles of the signal are different from the poles of the filter, then $y(k)$ can be divided into two parts. One part is generated by the poles of the signal, denoted by $y_x(k)$, while the other part arises from the poles of the filter, denoted as $y_h(k)$. Then it can be shown that $y_x(k)$ satisfies the following difference equation:

$$y(k) = \sum_{j=0}^{m} b_j x(j+k) - \sum_{i=1}^{n} a_i y(i+k). \quad (2.18)$$

Moreover,

$$y_x(k) = \sum_{i=1}^{M} A_i z_i^k, \quad (2.19)$$

where

$$A_i = R_i H(z_i). \quad (2.20)$$

Since this backward process starts at the end of the data sequence, or $k = N-1$, it requires that the initial conditions be zero, i.e., $x(k) \approx 0$, $y_x(k) \approx 0$, for $k \geq N$. To provide a backward process, independent of the poles of the filter, we must ensure that $y_h(k)$ be nonzero for $k \geq N$. This is achieved by placing the poles of the filter outside the unit circle. Because the backward process does not involve the poles of the filter, we place these poles (of the filter) outside the unit circle. This does not make the process unstable and guarantees that the poles of the signal are different from those of the filter.

As an example, consider the transfer function of the low-pass filter

$$H(z) = \frac{1}{1-qz} \quad \text{with} \quad q < 1, \quad (2.21)$$

we can write

$$y_i(k) = qy_i(k+1) + y_{i-1}(k), \quad i = 1, 2, \ldots, M. \quad (2.22)$$

Hence

$$y_i(k) = \sum_{j=1}^{M} \frac{R_j}{(1-qz_j)} z_j^k, \quad i = 1, \ldots, M. \quad (2.23)$$

The pencil-of-functions generated from y_i will be

$$\{y_{i-1}(k) - \lambda y_i(k)\} = \left\{ \sum_{j=1}^{M} R_j \frac{1-qz_j-\lambda}{1-qz_j^i} z_j^k \right\}, \quad (2.24)$$

and are linearly dependent if

$$\lambda = 1 - qz_i, \quad i = 1, 2, \ldots, M. \quad (2.25)$$

Hence, the poles must satisfy

$$\sum_{i=1}^{M+1} \sqrt{\Delta_{ii}} (qz-1)^{M-i+1} = 0. \quad (2.26)$$

Examples using this approach are presented in the literature [21,22].

(iii) Q Specified as a Band-Pass Filter

The selection of a band-pass filter makes it possible to estimate the poles of a signal with energy concentrated in a region other than the high or low end of the spectrum. Consider a cascade of two filters,

$$H_1(z) = \frac{1-qz}{1-q_1 z - q_2 z^2}, \quad (2.27)$$

and

$$H_2(z) = z,$$

so

$$y_1(t) = h_1(t) * y_0(t), \quad (2.28)$$

and

$$y_2(t) = h_2(t) * y_1(t).$$

By placing the poles of the band-pass filter outside the unit circle, we have

$$y_{2i-1}(k) = \sum_{j=1}^{M} R_i H_1^i(z_j) z_j^{k+i-1} \quad (2.29)$$

and

$$y_{2i}(k) = \sum_{j=1}^{M} R_i H_1^i(z_j) z_j^{k+1}, \quad i = 1, 2, \ldots, \frac{M}{2} \quad (2.30)$$

Here M is assumed to be even.

If the pencil-of-functions is defined by

$$\frac{y_1(k)}{H_1(\lambda)} - y_0(k), \quad y_2(k) - \lambda y_1(k), \ldots,$$

$$\frac{y_{M-1}(k)}{H_1(\lambda)} - y_{M-2}(k), \quad y_M(k) - \lambda y_{M-1}(k), \quad (2.31)$$

then

$$y_{2i}(k) - \lambda y_{2i-1}(k) = \sum_{j=1}^{M} R_j H_1^i(z_j)(z_j - \lambda) z_j^{k+i-1},$$

$$i = 1, 2, \ldots, \frac{M}{2}. \quad (2.32)$$

If λ is equal to one of the system poles, then the pencil becomes linearly dependent, as illustrated by Jain and Sarkar [23].

3. GENERALIZED PENCIL-OF-FUNCTION METHOD

With the advent of ESPRIT, it is clear that earlier methods for finding poles utilizing diagonal cofactors are quite inefficient. The generalized pencil-of-function method was developed utilizing the pencil-of-function concept and knowledge of the eigenvalues to find the poles, as in ESPRIT [25,26]. However, since the matrix pencil operates on the data directly, it can be applied when the noise is correlated (for example, due to multipath contamination) or colored.

Consider the general form of the signal to be

$$x(t) = \sum_{i-1}^{M} R_i e^{s_i t}. \quad (3.1)$$

The poles (s_i) are either real or occur in complex conjugate pairs. Additionally, they are stable ($\mathrm{Re}\{s_{ij}\} < 0$). The signal $x(t)$ is processed by a series of cascaded filters. The family of the signals $\{x(t), y_1(t), \ldots, y_M(t)\}$ are often called information signals. For convenience, the time variable t is dropped. The set of pencil-of-functions is now defined as

$$y_0 - \lambda y_1, \quad y_1 - \lambda y_2, \ldots, y_{M-1} - \lambda y_M, \quad (3.2)$$

where $y_0 = x$, $y_i = Q[y_{i-1}]$, $i = 1, \ldots, M$. $Q[\cdot]$ denotes the filtering function operating on the argument function. We assume $Q[\cdot]$ will only filter noise and will not significantly change the poles of the signal.

Since the functions $y_0, y_1, \ldots, y_{M-1}$ separately span a common M-dimensional subspace $\{\exp(s_i t), i = 1, 2, \ldots, M\}$, the functions $y_0, y_1, \ldots, y_{M-1}$ are linearly independent, while the functions $y_0, y_1, \ldots, y_M$ are linearly dependent. The linear independence of the set of pencil-of-functions $\{y_{i-1} - \lambda y_i, i = 1, 2, \ldots, M\}$ depends on the selection of λ.

For the noiseless data, we can define the $(N - L) \times L$ matrix pair Y_1, Y_2 as

$$Y_1 = \begin{bmatrix} x(1) & x(2) & \cdots & x(L) \\ x(2) & x(3) & \cdots & x(L+1) \\ \vdots & \vdots & & \vdots \\ x(N-L) & x(N-L+1) & \cdots & x(N-1) \end{bmatrix}, \quad (3.3)$$

$$Y_2 = \begin{bmatrix} x(0) & x(1) & \cdots & x(L-1) \\ x(1) & x(2) & \cdots & x(L) \\ \vdots & \vdots & & \vdots \\ x(N-L-1) & x(N-L) & \cdots & x(N-2) \end{bmatrix}, \quad (3.4)$$

where L is referred to as the pencil parameter [28,39].

It can be shown that

$$Y_1 = Z_1 R Z_0 Z_2, \quad (3.5)$$

$$Y_2 = Z_1 R Z_2, \quad (3.6)$$

where,

$$Z_1 = \begin{bmatrix} 1 & 1 & \cdots & 1 \\ z_1 & z_2 & \cdots & z_M \\ \vdots & \vdots & \vdots & \\ z_1^{(N-L-1)} & z_2^{(N-L-1)} & \cdots & z_M^{(N-L-1)} \end{bmatrix}, \quad (3.7)$$

and

$$Z_2 = \begin{bmatrix} 1 & z_1 & \cdots & z_1^{L-1} \\ 1 & z_2 & \cdots & z_2^{L-1} \\ \vdots & \vdots & \vdots & \\ 1 & z_M & \cdots & z_M^{L-1} \end{bmatrix}, \quad (3.8)$$

with

$$Z_0 = \mathrm{diag}[z_1, z_2, \ldots, z_M], \quad (3.9)$$

and

$$R = \mathrm{diag}[R_1, R_2, \ldots, R_M]. \quad (3.10)$$

Consider the matrix pencil given by

$$Y_1 - \lambda Y_2 = Z_1 R (Z_0 - \lambda I) Z_2. \quad (3.11)$$

One can show in general that the rank of $Y_1 - \lambda Y_2$ will be M, provided $M \leq L \leq N - M$. However, if $\lambda = z_i$, $i = 1, 2, \ldots, M$, the ith row of $Z_0 - \lambda I$ is zero, and the rank of $Z_0 - \lambda I$ will be $M - 1$. Here I is the identity matrix. Therefore, the matrix pencil $Y_1 - \lambda Y_2$ will also be reduced in rank to $M - 1$. By definition, the z_i's are the generalized eigenvalues (GEs) of the matrix pair $\{Y_1, Y_2\}$. Since both matrices in the pair span the same subspace, the GEs corresponding to

the common null space of the two matrices will be zero. Let the nonzero generalized eigenvalues of the matrix pair $\{Y_1, Y_2\}$ be λ_i, and the corresponding generalized eigenvectors be x_i, $i = 1, 2, \ldots, M$. Then

$$Y_1 x_i - \lambda_i Y_2 x_i = 0, \quad i = 1, 2, \ldots, M. \tag{3.12}$$

These equations can be combined to yield

$$Y_1 X = Y_2 \Lambda X, \tag{3.13}$$

where $\Lambda = \text{diag}\{\lambda_i, i = 1, 2, \ldots, M\}$, $X = \{x_i, i = 1, 2, \ldots, M\}$. Therefore,

$$Y_2^+ Y_1 = X^+ \Lambda X, \tag{3.14}$$

where Y_2^+ is the Moore–Penrose pseudoinverse of Y_2, which is defined as [27]

$$Y_2^+ = (Y_2^{\mathrm{H}} Y_2)^+ Y_2^{\mathrm{H}}. \tag{3.15}$$

The superscript "H" denotes the conjugate transpose operation.

From Eq. (3.5) and Eq. (3.6), the product $Y_2^+ Y_1$ can also be expressed as

$$Y_2^+ Y_1 = Z_2^+ Z_0 Z_2. \tag{3.16}$$

The exact eigenstructure of $Y_2^+ Y_1$ can be described as follows: If $M \leqslant L \leqslant N - M$, $Y_2^+ Y_1$ has M nonzero eigenvalues $\lambda_i = z_i$, $i = 1, 2, \ldots, M$, the ith corresponding right eigenvector equals the ith column of Z_2^+, and the ith corresponding left eigenvector equals the ith column of Z_2^{H}. The $L - M$ extraneous eigenvalues λ_i $(i \leqslant M + 1)$ equal zero and the corresponding right and left eigenvectors are in the null space of Z_2.

The pseudoinverse can be computed via the SVD. Based on the SVD theorem [37], the data matrix Y_2 is given by

$$Y_2 = U \Sigma V^{\mathrm{H}}, \tag{3.17}$$

where $U = [u_1, u_2, \ldots, u_M]$, $V = [v_1, v_2, \ldots, v_M]$, and $\Sigma = \text{diag}[\sigma_1, \sigma_2, \ldots, \sigma_M]$. u_i and v_i are, respectively, the ith left and right singular vectors of Y_2. $\sigma_1, \sigma_2, \ldots, \sigma_M$ are the singular values with $\sigma_1 \geqslant \sigma_2 \geqslant \cdots \geqslant \sigma_M$. Y_2^+ can be expressed as

$$Y_2^+ = \sum_{i-1}^{M} \frac{1}{\sigma_i} v_i u_i^{\mathrm{H}}. \tag{3.18}$$

For noisy data, Y_2 tends to be full rank. Therefore, Y_2 is replaced by $\hat{Y}_2$, which is a rank-M truncated approximation to Y_2, corresponding to the singular vector of the originally (in the noiseless case) zero singular values [38]. In general, the $L - M$ nonprincipal singular values are much smaller than the principal singular values. For the best least squares approximation, $\hat{Y}_2$, we set those $L - M$ smaller singular values to zero. Therefore,

$$\hat{Y}_2^+ = \sum_{i-1}^{M} \frac{1}{\hat{\sigma}_i} \hat{v}_i \hat{u}_i^{\mathrm{H}}. \tag{3.19}$$

Furthermore, this break in the singular values provides a method to detect the number of poles in the signal. For noisy data, the decay of the singular values becomes gradual, therefore it may be difficult to decide upon the number of principal singular values. By prefiltering, the difference between the principal and nonprincipal singular values is enhanced and the break will become more evident. This is illustrated through simulation.

It has been shown [27–34] that the MP technique is not only computationally more efficient, since the poles are found by a one step process, but they are also statistically more robust than the results given by the Tufts–Kumaresan method.

(i) The Band-Pass Matrix-of-Pencil (BPMP) Method for Pole Estimation [36,39]

Even though the MP method filters noise through a SVD of the data matrix by discarding nonprincipal singular vectors, noise still significantly impacts the principal singular values and vectors. Therefore, to further combat noise, prefiltering may be used prior to the SVD. One basic idea underlying the BPMP method is to first filter the data (digitally) to enhance the signal-to-noise ratio, then estimate the pole locations using the MP algorithm. Under these conditions, it can be shown that the BPMP method will out-perform the MP method.

To simplify the design procedure, we consider the use of a second-order IIR band-pass filter. The desired performance is obtained using a series of cascaded second-order filters. Since the input signal is modeled as a linear combination of sinusoids, the band-pass filter must pass a narrow band of sinusoidal signals whose radian frequencies are concentrated about a resonant frequency ω_0. This is achieved by locating the poles of the filter's transfer function, $H(z)$, in the vicinity of the poles of the input signal. We suppress undesired low and high frequency components by placing zeros at $z = 1$ and $z = -1$. Therefore, $H(z)$ is defined as

$$H(z) = K \frac{(z + 1)(z - 1)}{(z - re^{j\omega_0})(z - re^{-j\omega_0})}, \tag{3.20}$$

where K is a constant selected to control the gain of the filter.

To obtain a difference equation describing the filter, we write $H(z)$ in canonical form. That is,

$$H(z) = K' \frac{1 - z^2}{1 - q_1 z - q_2 z^2}, \tag{3.21}$$

where

$$q_1 = \frac{2 \cos \omega_0}{r}, \tag{3.22}$$

and

$$q_2 = \frac{1}{r^2}. \tag{3.23}$$

K' is chosen so that the filter has a unit gain at $\omega = \omega_0$.

To control the width of the pass-band of the filter, we introduce another parameter, BW, such that

$$r = \frac{1}{1 - \mathrm{BW}}, \quad \mathrm{BW} > 0. \tag{3.24}$$

Substituting Eq. (3.24) into (3.22) and (3.23), we have

$$q_1 = 2(1 - \mathrm{BW}) \cos \omega_0, \tag{3.25}$$

$$q_2 = (1 - \mathrm{BW})^2. \tag{3.26}$$

Provided that both the number of samples, N, and the damping factors are large enough, $x(k)$ and $y_x(k)$ are approximately zero when k is larger that N. We obtain

$$y(N-1) \approx K'x(N-1), \tag{3.27}$$

$$y(N-2) \approx q_1 y(N-1) + K'x(N-2), \tag{3.28}$$

$$y(k) = q_2 y(k+2) + q_1 y(k+1) + K'[x(k) - x(k+2)], \quad \text{for} \quad 0 \leq k \leq N-3. \tag{3.29}$$

Thus, the output of the processing filter, $y(k)$, contains only the poles of the input signal.

To provide the desired response, a cascaded band-pass filter is implemented. Assuming the number of the filters is d, and denoting the output of the dth filter as $y^{(d)}(k)$, then we can use $y^{(d)}(k)$ to form the matrix pair Y_1 and Y_2. The poles of the signal are obtained from the eigenvalues of $Y_2^+ Y_1$.

The central frequency, ω_0, and bandwidth, BW, are selected based upon analysis of spectral (FFT) data. That is, ω_0 and BW are computed based upon the spectral peak and width of the input signals. Based upon simulation analysis, we found that the choices of ω_0 and BW are not critical for moderate to high values of the signal-to-noise ratio.

It is well-known that IIR filtering usually is more efficient than FIR filtering due to the utilization of recursive relationships. However, the IIR filter can only be used for the signals which contain exponentially damped sinusoidal signals. Besides, there is always a truncation error associated with the backward process associated with IIR filtering. When the number of samples, N, and the damping factors are small, the assumption $x(k) \approx 0$, $y(k) \approx 0$ for $k \geq N$ no longer holds. To apply the BPMP method to such signals, FIR filtering must also be exploited.

The first step is to find the impulse response of the filter. From the magnitude of the FFT of the signal, the cutoff frequencies of the band-pass filter ω_L, $\omega_U (\omega_L < \omega_U)$ can be found. The impulse response of the desired band-pass filter is defined as

$$h_d(n) = \frac{1}{2\pi} \int_{\Omega} H(e^{j\omega}) e^{jn\omega} d\omega, \tag{3.30}$$

where Ω is the region in the frequency domain where the signal lies. For a real signal with the cutoff frequencies ω_L and ω_U, the impulse response of the desired band-pass filter can be found as

$$h_d(n) = \frac{1}{n\pi} [\sin(\omega_U n) - \sin(\omega_L(n)], \quad n = \pm 1, \pm 2, \ldots, \tag{3.31}$$

$$h_d(0) = \frac{\omega_U - \omega_L}{\pi}. \tag{3.32}$$

Then the truncated finite impulse response is given by

$$h(n) = h_d(n) w(n), \quad n = 0, \pm 1, \ldots, \pm \frac{q-1}{2}, \tag{3.33}$$

where q is the length of the band-pass filter, and $w(n)$ is the window function. q is assumed to be odd.

Generally, the second step is to perform FIR filtering by using linear convolution. Even though FIR filtering will not increase the number of poles in the filtered data, the filtered data used to form the matrix pair Y_1 and Y_2 will be reduced by using linear convolution [19]. Thus, a reduction in the number of samples will affect the efficiency of the SVD filter. To maintain the performance of the SVD filtering, we introduce a prefiltering approach by using circular convolution.

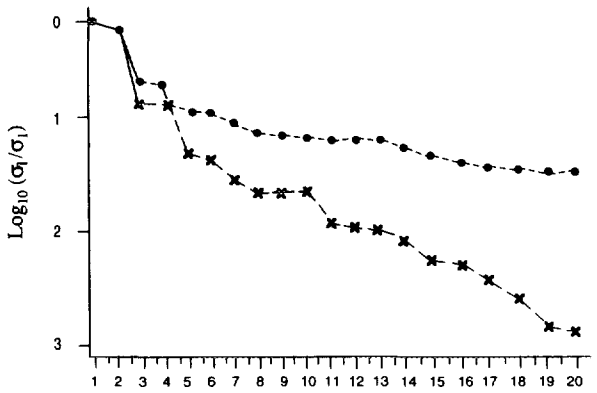

FIG. 1. The singular values of the data matrix Y_2 (●) without filtering; (×) after filtering.

Basically, circular convolution is to form an $(N - L) \times (N - L)$ filtering matrix by using the impulse response of the filter. If $N - L$ is odd, the filter length is taken as $N - L$. The first row of H is the reverse version of $h(n)$. The other rows of H are formed using the circular right shift of the previous row. That is,

$$H = \begin{bmatrix} h\left(\frac{q-1}{2}\right) & h\left(\frac{q-3}{2}\right) & \cdots & h\left(-\frac{q-1}{2}\right) \\ h\left(-\frac{q-1}{2}\right) & h\left(\frac{q-1}{2}\right) & \cdots & h\left(-\frac{q-3}{2}\right) \\ \vdots & \vdots & & \vdots \\ h\left(\frac{q-3}{2}\right) & h\left(\frac{q-5}{2}\right) & \cdots & h\left(\frac{q-1}{2}\right) \end{bmatrix} \tag{3.34}$$

If $N - L$ is even, the filter length is chosen as $N - L - 1$ with zero padding one sample.

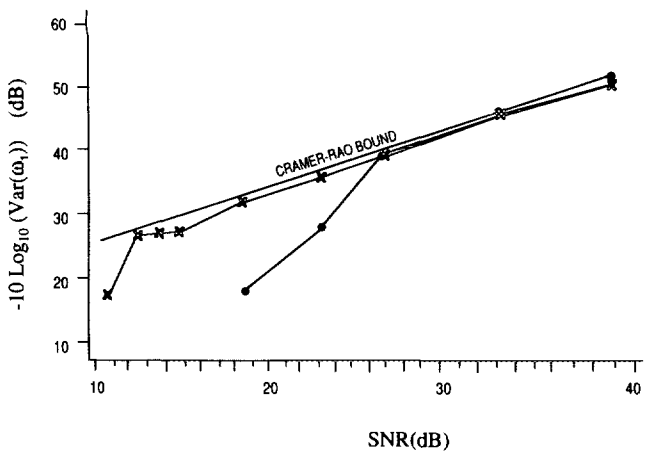

FIG. 2. The inverted sample variance of ω_1 versus SNR (IIR filtering) BW = 0.1, $\omega_U = 0.8796$, $N = 50$, $L = 20$, $d = 1$: (●) MP; (×) BPMP.

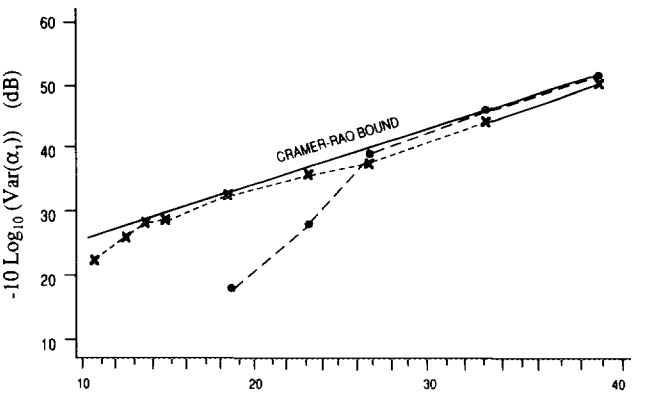

FIG. 3. The inverted sample variance of α_1 versus SNR (IIR filtering) BW = 0.1, $\omega_U = 0.8796$, $N = 50$, $L = 20$, $d = 1$: (●) MP; (×) BPMP.

Premultiplying both Y_1 and Y_2 by H, we have

$$Y_1' = HY_1 = [y_1', y_2', \ldots, y_L'], \tag{3.35}$$

$$Y_2' = HY_2 = [y_0', y_1', \ldots, y_{L-1}'], \tag{3.36}$$

where

$$y_i' = Hy_i, \tag{3.37}$$

and

$$y_i = [y(i), y(i+1), \ldots, y(i+N-L-1)]^T. \tag{3.38}$$

From Eq. (3.37), one can observe that y_i' arises from the circular convolution between $h(n)$ and y_i. Therefore, the filtered matrices, Y_i''s, are "cleaner" than the original.

In the noise free case, substituting Eq. (3.5), Eq. (3.6) into Eq. (3.35), Eq. (3.36), respectively, one obtains

$$Y_1' = HZ_1RZ_0Z_2, \tag{3.39}$$

$$Y_2' = HZ_1RZ_2. \tag{3.40}$$

Let $Z_1' = HZ_1$, then

$$Y_1' = Z_1'RZ_0Z_2, \tag{3.41}$$

$$Y_2' = Z_1'RZ_2. \tag{3.42}$$

Since the rank of H is not less than M, the rank of Z_1' is M. Therefore,

TABLE 1

The Mean-Squared Error and the Bias of ω_1 for Different BW (SNR = 18.3 dB)

BW	0.001	0.01	0.05	0.1	0.3
MSE	6.43×10^{-4}	6.46×10^{-4}	6.98×10^{-4}	7.56×10^{-4}	1.32×10^{-3}
Bias	0.0016	0.0006	−0.0019	−0.0044	−0.0097

$$Z_1'Z_1' = I. \tag{3.43}$$

From Eq. (3.41), Eq. (3.42), and Eq. (3.43), it turns out that

$$Y_2'^{+}Y_1' = Z_2^{+}Z_0Z_2. \tag{3.44}$$

Therefore, the signal poles remain in the eigenvalues of $Y_2'^{+}Y_1'$. For the noisy data, the matrix pair $\{Y_1', Y_2'\}$ is more robust with respect to noise than the matrix pair $\{Y_1, Y_2\}$ because of the filtering process.

(ii) Performance Analysis of the BPMP Method

In this section, computer simulation results illustrate the performance of the BPMP method. In the simulation analysis, exponentially damped sinusoidal signals are utilized. Since the input signals are real, we have

$$\begin{aligned} y(k) &= x(k) + n(k) \\ &= \sum_{i=1}^{M/2} b_i e^{-\alpha_i k}\sin(\omega_i k + \phi_i) + n(k), \\ &\qquad k = 0, 1, \ldots, N-1, \end{aligned} \tag{3.45}$$

where $n(k)$ is zero-mean Gaussian white noise with variance σ^2. For convenience, the sampling period T_s has been set equal to 1 in Eq. (3.30). The signal-to-noise ratio (SNR) is defined as

$$\mathrm{SNR(dB)} = 10 \log_{10} \frac{\sum_{k=0}^{N-1} x^2(k)}{N\sigma^2}. \tag{3.46}$$

The simulations were conducted using double precision mathematics, on a VAX8820 programmed in FORTRAN 77. The International Mathematics and Statistics Library (IMSL) routine, GGNML, was used to generate the pseudo noise process. The IMSL routines LSVD and EIGRF were used for SVD and eigen-decomposition.

In the first example, consider an input signal with the following parameters, $M = 4$, $\omega_1 = 1.26\pi$, $\omega_2 = 0.3\pi$, $\alpha_1 = \alpha_2 = 0.1$, $b_1 = b_2 = 1$, $\phi_1 = \phi_2 = 0$, and $N = 50$. An IIR band-pass filter is selected with central frequency ω_0 and bandwidth BW $= 0.1\omega_0$. Also, one filter is selected ($d = 1$). The matrix-pencil parameter, L, equals 20. The truncated error is 1.1453×10^{-2} for the noise free case.

Now consider data with one noise realization (SNR = 18.3 dB). The singular values of the matrix Y_2 are shown in Fig. 1. Without filtering, the singular values break at the third value, meaning that the third and fourth singular values are immersed in the noise. After prefiltering, it is clear that the break occurs between the fourth and fifth singular values. To obtain the sample variance of the estimate of ω_1, 200 trials are performed. The noise for each run is independent. In comparison to the BPMP method, we compute the Cramer–Rao Lower Bound (CRLB) of the variance of the angular frequency estimate, as given by an unbiased estimator using the method given by Hua [18]. The inverse of the sample variance of the estimate of ω_1, and the corresponding CRLB versus SNR are plotted in Fig. 2. For comparison, the sample variance of the estimate of ω_1 obtained by the MP method is also shown in Fig. 2. It is clear that the MP method performs better than the BPMP method at high SNR. The inverted sample variance of α_1-plotted in Fig. 3 demonstrates that the BPMP method is better than the MP method, especially at low SNRs. In Table 1, we tabulate the mean-squared error and the bias of ω_1, for BW ranging from 0.001 to 0.3. One can see that both the mean-squared error and the bias increase as the bandwidth of the filter becomes wider, and more noise energy passes through the filter. The mean-squared error and the bias of ω_1 are marginal when BW is less than 0.1, and they are given in Table 2. It is understandable that both the mean-squared error and the bias of ω_1 become smaller when ω_0 is close to ω_1.

To determine the performance of the FIR filter, the exponentially damped sinusoidal signal with small values of both N and damping factors are used in a simulation analysis. The parameters are $N = 30$, $M = 4$, $\omega_1 = 0.2\pi \approx 0.628$, $\omega_2 = 0.35\pi \approx 1.1$, $\alpha_1 = 0.02\pi$, $\alpha_2 = 0.035\pi$, $b_1 = b_2 = 1$, and $\phi_1 = \phi_2 = 0$. This is the same example presented by Hua and Sarkar [29]. L is set equal to 10, and $N - L$ equals 20. The low cutoff frequency, ω_L, and the high cutoff frequency, ω_U, are chosen as 0.5 and 1.2, respectively. The window function is Kaiser with $B = 5.658$ [41]. That is,

TABLE 2

The Mean-Squared Error and the Bias of ω_1 for Different ω_0 (SNR = 18.3 dB)

ω_0	0.7796	0.8168	0.8796	0.9424	0.9796
MSE	1.32×10^{-3}	9.21×10^{-4}	7.56×10^{-4}	8.92×10^{-4}	1.21×10^{-3}
Bias	0.0104	0.0038	−0.0044	−0.0137	−0.0222

$$w(n) = \frac{I_0(\beta\sqrt{1 - [2n/(N-1)]^2})}{I_0'(\beta)}, \quad -\frac{N-1}{2} \leq n \leq \frac{N-1}{2}, \tag{3.47}$$

where

$$I_0(x) = 1 + \sum_{k=1}^{\infty} \left[\frac{(x/2)^k}{k!}\right]^2. \tag{3.48}$$

The length of the FIR filter is chosen as 19. Then the filtering matrix is formed by using the impulse response of the filter. Monte-Carlo simulations were conducted with 200 runs. The inverted sample variances of the estimate of ω_1 versus SNR are shown in Fig. 4. From the plot of Fig. 4, it is evident that the BPMP method performs better than the MP method. The improvement of the BPMP method ranges from 2.5 to 10 dB.

It is thus seen that the performance of the BPMP is quite close to the Cramer–Rao Bound.

4. REAL-TIME IMPLEMENTATION OF THE BPMP METHOD

VLSI microelectronics technology and computer-aided design methodologies are precipitating a revolution in signal processing, enabling real-time implementation of the BPMP method. The relationships between VLSI and modern signal processing algorithm design is intimate. The ever-increasing demands on it improved performances of modern signal processing algorithms require tremendous computational capability in terms of both throughput and memory. The availability of low cost, high density, high speed VLSI devices has spawned a new era for implementing sophisticated algorithms which run in real-time. These devices have advanced architectures, dedicated Digital Signal Processing (DSP) instruction sets, and they execute millions of operations per second.

(i) Enabling Technology: The DSP32C Processor

The DSP32C digital signal processor is one of the newest member of the AT&T family of 32-bit floating point processors [42–46]. They were developed in 1988, and are commercially available. This processor is especially suitable for applications requiring floating-point arithmetic, high throughput, large memory, and low power dissipation. It is fabricated using CMOS technology, and executes a single multiply and accumulate in 70 ns. The C-like syntax of the DSP32 Assembly Language makes this processor very attractive. Many existing algorithms developed for use on mainframe computers and array processors are easily converted for use on a DSP32C processor.

(ii) Real-Time Implementation of BPMP on a DSP32C Processor

For the BPMP method, the primary steps include a SVD of the $(N \times L) \times (L + 1)$ data matrix Y and eigenvalue decomposition of an $M \times M$ matrix $V_2^H(V_1^H)^+$. It is easy to show that the SVD and eigen-decomposition yield the same subspace estimate of V, which is a matrix with the right singular vectors of Y. That is,

$$Y^H Y = V\Sigma^2 V^H. \tag{4.1}$$

Conversely, the right singular vector of Y can be found from the eigenvectors of $Y^H Y$. These techniques are equivalent in the absence of errors due to finite precision when computing the decomposition.

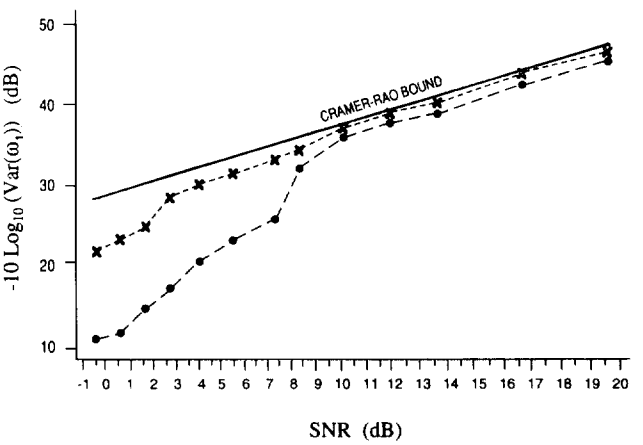

FIG. 4. The inverted sample variance of ω_1 versus SNR (FIR filtering) $L = 10$, $q = 19$, $\omega_L = 0.5$, $\omega_U = 1.2$, $\beta = 5.658$, Kaiser window: (●) MP; (×) BPMP.

TABLE 3

The Estimated Result for the Implementation of the Matrix-Pencil (MP) Method

SNR (dB)	α_1	ω_1	α_2	ω_2	Computational time (ms)
∞	0.06282800	0.62832969	0.10995562	1.09956603	50
3.96	0.08428995	0.60196537	0.07915761	1.10879159	50
	$\Delta = 34\%$	$\Delta = 4.2\%$	$\Delta = 28\%$	$\Delta = 0.84\%$	

However, the computational differences are significant. The full SVD of Y is on the order of $[(N-L)\times(L+1)^2]$, which can be significantly larger than the $O(L+1)^3$ operations required for eigen-decomposition of Y^HY. One major advantage of the SVD over eigen-decomposition is due to dynamic range, that is, data may be processed directly without squaring. Thus, numerical problems associated with ill-conditioned matrices are mitigated to some extent by use of the SVD. For real-time implementation, a reduction in computation time is often more important than precision. Hence, the subspace estimate of V obtained through eigen-decomposition is most suitable for real-time implementation.

The subroutine for computing the eigenvalues of a real nonsymmetric matrix includes three steps. First, the matrix needs to be balanced [47]; second, the balanced matrix is reduced to real upper-Hessenberg form [48]; and third, the shift QR algorithm is used to compute the eigenvalues of the Hessenberg matrix [49,50].

Balancing reduces the 1-norm of the original matrix whenever sums of the magnitudes of elements in a given row and (corresponding) column are remarkably different, while at the same time leaving the eigenvalues unchanged. The sums of the magnitudes of elements in corresponding rows and columns are made nearly equal by exact similarity transformations, and eigenvalues are isolated by permitting similarity transformations. The advantage of balancing is improved accuracy when computing eigenvalues and eigenvectors, whenever the sums of the magnitudes of elements in the row and corresponding column are quite different.

The DSP32C code for the BPMP method is executed on an IBM AT with a PC-32C board, which consists of an AT&T WE-DSP32C-80 digital signal processor, with 256 kbytes on-board static RAM, and a 16 Mbit/s. buffered bidirectional serial port. The highest transfer rate is 3 Mbytes/s. Additionally, up to 16 Mbytes of external memory can be directly addressed by the external memory interface.

The execution program is downloaded and executed on the PC-32C board via utility software subroutines D3EMU. In experiments for evaluation of the BPMP method, synthetic data was used. For convenience, the data parameters included, $N = 30$, $M = 4$, $\omega_1 = 0.2\pi$, $\omega_2 = 0.35$, $\alpha_1 = 0.02\pi$, $\alpha_2 = 0.035\omega$, $b_1 = b_2 = 1$, and $\phi_1 = \phi_2 = 0$. The first step is to form the Hankel data matrix, Y, with 11 columns ($L = 10$). The subroutine EIRS computes the eigenvectors of Y^TY. The matrices V_1 and V_2 are formed from the eigenvectors Y^TY. The next step is to compute the poles of the signal from the eigenvalues of $V_2^H(V_1^H)^+$. Since the signal is real, the poles are either real or complex conjugate. The poles of the signal can be computed from the eigenvalues of $V_1^+V_2$ by invoking the subroutine EIRF. Finally, damping factors and the angular frequencies are calculated using the equations

$$\hat{\alpha}_i = \frac{-1}{2}\ln(\mathrm{Re}^2(\hat{z}_i) + \mathrm{Im}^2(\hat{z}_i)) \tag{4.2}$$

$$\hat{\omega}_i = \tan^{-1}(\mathrm{Im}(\hat{z}_i)/\mathrm{Re}(\hat{z}_i)), \tag{4.3}$$

where $\hat{z}_i$ is the estimate of the poles of the signal.

For the BPMP method, the first column of Y is used to form the filtering matrix H. Since H is circulant, we need to store only one row. Once the filtered matrix $Y'(=HY)$ is generated, the remaining steps are the same as in the Matrix Pencil (MP) method. The result for the MP method is listed in Table 3, and the result for the BPMP method is given in Table 4. The relative error for the estimate x is defined as

$$\Delta = \frac{|x(\mathrm{SNR}=\infty) - x(\mathrm{SNR} = 3.96\ \mathrm{dB})|}{x(\mathrm{SNR}=\infty)} \times 100\%. \tag{4.4}$$

Comparing the results in Tables 3 and 4, one observes a significant reduction of the relative errors after the prefiltering process. The computation time required for the BPMP method is longer than for the MP method. However, this is the cost of improved accuracy.

TABLE 4

The Estimated Result for the Implementation of the Band-Pass Matrix-Pencil (BPMP) Method

SNR (dB)	α_1	ω_1	α_2	ω_2	Computational time (ms)
∞	0.06282903	0.62832952	0.1099597	1.09956515	50
3.96	0.06274100	0.62216312	0.09921833	1.12093556	60
	Δ = 0.14%	Δ = 0.98%	Δ = 9.8%	Δ = 1.9%	

5. CONCLUSION

The matrix pencil approach has been presented from a historical perspective and its performance has been compared to other contemporary techniques. The Band-Pass Matrix-Pencil method has been implemented in real time on an AT&T DSP32C chip. Typical results are presented for real time implementation of the Matrix-Pencil and the Band-Pass Matrix-Pencil technique. The small relative errors when estimating parameters, and reasonable computation time demonstrates the promising future for real-time Matrix-Pencil-based algorithms.

APPENDIX

```
C-----PROGRAM FOR POLES RETRIEVAL FROM
      REAL DATA SEQUENCE
C-----BY USING GENERALIZED PENCIL-OF-
      FUNCTIONS METHOD.
C-----PARAMETERS:
C-----ND IS NUMBER OF DATA SAMPLES.
C-----NP IS NUMBER OF POLES. (TO BE
      ESTIMATED FROM THE SINGULAR VALUES)
C-----AR ARE DAMPING FACTORS.
C-----W ARE ANGULAR FREQUENCIES.
C-----ASSUME THAT ND<=150,NP<=75 AND
      L<=75.
      REAL WK(10000),AR(75),W(75)
      REAL
      Y(150),YY1(150,150),YY2(150,150),
      SYY1(75,75)
      REAL SYY2(75,75),BETA(75),TR
      COMPLEX
      Z(75),ZY(75,75),ALFA(75),TC
      IIR=75
      OPEN(UNIT=20,FILE='SIGNAL.DAT',
      STATUS='OLD')
      OPEN(UNIT=21,FILE='GPOFR.DAT',
      STATUS='NEW')
      WRITE(6,1122)
1122  FORMAT(1X,'INPUT ND,NP,L:')
C-----L IS A PENCIL PARAMETER : NP < L < N/2,
      L = N/2 - 1 is suggested )
      READ(5,2211) ND,NP,L
2211  FORMAT(I4)
C-----INPUT SIGNAL. Y(I) IS THE DATA
      SEQUENCE TO BE APPROXIMATED BY
C-----NP EXPONENTIALS
      READ(20,1111) (Y(I),I=1,ND)
1111  FORMAT(2E)
      NL=ND-L
      DO 50 I1=1,NL
      DO 50 I2=1,L
      YY1(I1,I2)=Y(I1=I2-1)
50    YY2(I1,I2)=Y(I1+I2)
      DO 15 I1=1,L
      DO 15 I2=1,L
      SYY1(I1,I2)=0.
      SYY2(I1,I2)=0.
      DO 15 K=1,NL
      SYY1(I1,I2)=SYY1(I1,I2)+YY1(K,
      I1)*YY1(K,I2)
15    SYY2(I1,I2)=SYY2(I1,I2)+YY1(K,
      I1)*YY2(K,I2)
C-----CALL AN IMSL ROUTINE TO COMPUTE
      GENERALIZED EIGENVALUES.
      CALL EIGZF(SYY2,IIR,SYY1,IIR,L,2,
      ALFA,BETA,ZY,IIR,WK,IER)
      WRITE(6,7777) IER,W(1)
7777  FORMAT(1X,'IER=',I4,2X,'W(1)=',
      E12.5)
C-----ORDER BETA.
      DO 25 I1=1,L-1
      DO 26 I2=I1+1,L
      IF(ABS(BETA(I1)).GE.ABS
      (BETA(I2))) GOTO 26
      TR=BETA(I1)
      TC=ALFA(I1)
      BETA(I1)=BETA(I2)
      ALFA(I1)=ALFA(I2)
      BETA(I2)=TR
      ALPHA(I2)=TC
26    CONTINUE
25    CONTINUE
      WRITE(6,8888) (I1,BETA(I1),I1=1,L)
```

```
8888    FORMAT(1X,I3,1X,'BETA=',E12.5)
        DO 35 I1=1,NP
35      Z(I1)=ALFA(I1)/BETA(I1)
C-----SORT RESULTS.
        DO 140 I=1,NP
        AR(I)=REAL(CLOG(Z(I)))
        W(I)=AIMAG(CLOG(Z(I)))
140     CONTINUE
        DO 120 IM=1,NP-1
        IF(NP.EQ.1) GOTO 120
        DO 130 JM=IM+1,NP
        IF(AR(IM).LT.AR(JM)) GOTO 130
        T1=AR(IM)
        AR(IM)=AR(JM)
        AR(JM)=T1
        T1=W(IM)
        W(IM)=W(JM)
        W(JM)=T1
130     CONTINUE
120     CONTINUE
        WRITE(21,1313) ND,NP,L
1313    FORMAT(1X,'ND,NP,L=',3I4)
        WRITE(21,1212)
        (I,AR(I),W(I),I=1,NP)
1212    FORMAT(1X,I3,2X,'(AR,W)=',2E12.5)
        STOP
        END
```

REFERENCES

1. Baum, C. E. On the singularity expansion method for the solution of electromagnetic interaction problems. EMP Interaction Note 8, Air Force Weapons Laboratory, Kirkland AFB, New Mexico, Dec. 11, 1971.
2. Marin, L., and Latham, R. W. Representation of transient scattered fields in terms of free oscillations of bodies. *Proc. IEEE* **60** (May 1972), 640–641.
3. Tesche, F. M. On the analysis of scattering and antenna problems using the singularity expansion technique. *IEEE Trans. Antennas and Propagation* **AP-21**, No. 1 (Jan. 1973), 53–62.
4. Pearson, L. W., VanBlaricum, M. L., and Mittra, R. "A new method for radar target recognition based on the singularity expansion for the target," *Record of the IEEE 1975 Int. Radar Conf.*, Arlington, Virginia, April 1975, pp. 452–457.
5. Moffatt, D. L., and Mains, R. K. Detection and discrimination of radar target. *IEEE Trans. on Antennas and Propagation* **AP-23** (May 1975), 358–367.
6. Sarkar, T. K., Nebat, J., Weiner, D. D., and Jain, V. K. A discussion of various approaches to the identification/approximation problem. *IEEE Trans. Antennas and Propagation* (Jan. 1982), 89–98.
7. Prony, R. Essai experimental et analytique . . . *Paris J. l'Ecola Polytechnique* **1**, Calvier 2, 24–76. (1795).
8. Hilderband, F. B. *Introduction to numerical analysis.* McGraw–Hill, New York, 1956, pp. 378–382.
9. VanBlaricum, M. L., and Mittra, R. A technique for extracting the poles and residues of a system directly from its transient response. *IEEE Trans. Antennas and Propagation* **AP-23** (Nov. 1975), 777–781.
10. VanBlaricum, M. L., and Mittra, R. Problems and solutions associated with Prony's method for processing transient data. *IEEE Trans. Antennas and Propagation* **AP-26** (Jan. 1978), 174–182.
11. Tufts, D. W., and Kumaresan, R. Frequency estimation of multiple sinusoids: making linear prediction perform like maximum likelihood. *Proc. IEEE* **70** (Sept. 1982), 975–989.
12. Kumaresan, R., and Tufts, D. W. Estimating the parameters of exponentially damped sinusoids and pole-zero modelling in noise. *IEEE Trans. Acoust. Speech Signal Process.* **ASSP-30** (Dec. 1982), 833–840.
13. Gantmacher, F. R. *Theory of Matrices,* Vol. I. Chelsea, New York, 1960.
14. Jain, V. K., and Gupta, R. D. Identification of linear systems through a Grammian technique. *Int. J. Control* **12**, No. 3 (1970), 421–431.
15. Jain, V. K. Filter analysis by grammian method. *IEEE Trans. Audio Electrocoustic* **AU-21** (1973), 120–123.
16. Jain, V. K. Filter analysis by use of pencil-of-functions: Part I. *IEEE Trans. Circuits and Systems* **CAS-21** (Sept. 1974), 574–579.
17. Jain, V. K. Filter analysis by use of pencil-of-functions: Part II. *IEEE Trans. on Circuits and Systems* **CAS-21** (Sept. 1974), 580–583.
18. Hua, Y. On techniques for estimating parameters of exponentially damped/undamped sinusoids in noise. Ph.D. dissertation, Syracuse University, Syracuse, New York, Aug. 1988.
19. Hu, F. The band pass matrix pencil method for parameter estimation of exponentially damped/undamped sinusoidal signals in noise. Ph.D. Dissertation, Syracuse University, Syracuse, New York, Dec. 1990.
20. Sarkar, T. K., Nebat, J. N., Weiner, D. D., and Jain, V. K. Suboptimal approximation/identification of transient waveforms from electromagnetic systems by pencil-of-function method. *IEEE Trans. Antennas and Propagation* **37**, No. 2 (Feb. 1989), 229–234.
21. Jain, V. K., Sarkar, T. K., and Weiner, D. D. Rational modelling by the pencil-of-functions method. *IEEE Trans. Acoust. Speech Signal Process.* **ASSP-31** (June 1983), 564–573.
22. Mackay, J. A., and McCowen, A. An improved pencil-of-functions method and comparisons with traditional methods of pole extraction. *IEEE Trans. Antennas and Propagation* **AP-35** (Apr. 1987), 435–441.
23. Jain, V. K., and Sarkar, T. K. High performance signal modelling by pencil-of-function method. *IEEE Trans. Acoust. Speech Signal Process.* **ASSP-34** (Aug. 1986), 997–1000.
24. Jain, V. K., and Sarkar, T. K. Multivariable system identification by pencil-of-functions method. *IEEE Trans. Instrum. and Meas.* **IM-34** (Dec. 1985), 550–557.
25. Roy, R., Paulraj, A., and Kailath, T. ESPRIT—A subspace rotation approach to estimation of parameters of cisoids in noise. *IEEE Trans. Acoust. Speech Signal Process.* **ASSP-34** (Oct. 1986), 1340–1342.
26. Roy, R., and Kailath, T. ESPRIT—Estimation of signal parameters via rotational invariance techniques. *IEEE Trans. on Acoust. Speech Signal Process.* **ASSP-37,** No. 7 (July 1989), 984–995.
27. Hua, Y., and Sarkar, T. K. Perturbation analysis of TK method for harmonic retrieval problems. *IEEE Trans. Acoust. Speech Signal Process.* **36,** No. 2 (Feb. 1988), 228–240.
28. Ouibrahim, H., Weiner, D. D., and Sarkar, T. K. Matrix pencil approach to direction finding. *IEEE Trans. Acoust. Speech Signal Process.* **36** (Apr. 1988), 610–612.
29. Hua, Y., and Sarkar, T. K. Generalized pencil-of-function method for extracting poles of an EM system from its tran-

sient response. *IEEE Trans. Antennas and Propagation* **37**, No. 2 (Feb. 1989), 229–234.

30. Hua, Y., and Sarkar, T. K. Matrix pencil method for estimating parameters of exponentially damped/undamped sinusoids in noise. *IEEE Trans. Acoust. Speech Signal Process.* **38**, No. 5 (May 1990), 814–824.
31. Hua, Y., and Sarkar, T. K. Matrix pencil and system poles. *Signal Process.* **21**, No. 2 (Oct. 1990), 195–198.
32. Hua, Y., and Sarkar, T. K. A perturbation property of the TLS-LP method. *IEEE Trans. Acoust. Speech Signal Process.* **38** (Nov. 1990), 2004–2005.
33. Hua, Y., and Sarkar, T. K. On the total least squares linear prediction method for frequency estimation. *IEEE Trans. Acoust. Speech Signal Process.* **38** (Dec. 1990), 2186–2189.
34. Hua, Y., and Sarkar, T. K. On SVD for estimating generalized eigenvalues of singular matrix pencil in noise. *IEEE Trans. Signal Process.* **39**, No. 4 (Apr. 1991), 892–900.
35. Hua, Y., and Sarkar, T. K. Parameter estimation of multiple transient signals. *Signal Process.* **28** (1992), 109–115.
36. Hu, F., Sarkar, T. K., and Hua, Y. Utilization of bandpass filtering from the matrix pencil method. *IEEE Trans. Signal Process.* **41**, No. 1 (Jan. 1993), 442–446.
37. Golub, G. H., and Van Loan, C. F. *Matrix Computations.* John Hopkins Univ., Baltimore, 1983.
38. Wilkinson, J. H. *The Algebraic Eigenvalue Problem.* Clarendon, Oxford, 1965.
39. Hu, F., Sarkar, T. K., and Hua, Y. The spectrum parameter estimation by using prefiltering and matrix pencil method. *The 5th ASSP Workshop on Spectrum Estimation and Modelling,* 1990. [Also, Hu, F. The band-pass matrix pencil method for parameter estimation of exponentially damped/undamped sinusoidal signals in noise. Ph.D. Thesis, Syracuse University, Nov. 1990]
40. Rife, D. C., and Boorstyn, R. R. Multiple tone parameter estimation from discrete time observations. *Bell System Tech. J.* (Nov. 1976), 1389–1410.
41. Rabiner, L. R., and Gold, B. *Theory and Application of Digital Signal Processing.* Prentice–Hall, Englewood Cliffs, N.J., 1975.
42. AT&T. *WE@DSP32 Digital Signal Processor Information Manual,* Dec. 1986.
43. AT&T. *WE@DSP32C Digital Signal Processor Advance Information Data Sheet,* Aug. 1987.
44. AT&T. *WE@DSP32 and DSP32C Support Software Library User Manual,* Aug. 1987.
45. AT&T. *WE@DSP32-AL Application Software Library Reference Manual,* Aug. 1987.
46. AT&T. *D3EMU, Software Debugger for the AT&T WE-DSP32 and DSP32C Digital Signal Processors,* 1990.
47. Parlett, B. N., and Reinsch, C. Balancing a matrix for calculation of eigenvalues and eigenvectors. *Numer. Math.* **13** (1969), 293–304.
48. Martin, R. S., and Wilkinson, J. H. Similarity reduction of a general matrix to Hessenberg form. *Numer. Math.* **12** (1968), 349–368.
49. Martin, R. S., Peters, G., and Wilkinson, J. H. The QR algorithm for real Hessenberg matrices. *Numer. Math.* **14** (1970), 219–231.
50. Francis, J. C. The QR transformation—a unitary analogue to the LR transformation. *Comput. J.* **4** (1961/62), 265–271 and 332–345.

TAPAN KUMAR SARKAR was born in Calcutta, India, on August 2, 1948. He received the B. Tech. degree from the Indian Institute of Technology, Kharagpur, India, in 1969, the M.Sc.E. degree from the University of New Brunswick, Fredericton, Canada, in 1971, and the M.S. and Ph.D. degrees from Syracuse University, Syracuse, New York, in 1975. From 1975 to 1976 he was with the TACO Division of the General Instruments Corporation. He was with the Rochester Institute of Technology, Rochester, NY, from 1976 to 1985. He was a Research Fellow at the Gordon McKay Laboratory, Harvard University, Cambridge, MA, from 1977 to 1978. He is now a professor in the Department of Electrical and Computer Engineering, Syracuse University, Syracuse, NY. His current research interests deal with numerical solutions of operator equations arising in electromagnetics and signal processing with application to system design. He obtained one of the "best solution" awards in May 1977 at the Rome Air Development Center (RADC) Spectral Estimation Workshop. He has authored or coauthored more than 154 journal articles and conference papers and has written chapters in eight books. Dr. Sarkar is a registered professional engineer in the State of New York. He received the Best Paper Award of the IEEE Transactions on Electromagnetic Compatibility in 1979. He was an Associate Editor for feature articles of the *IEEE Antennas and Propagation Society Newsletter,* and he was the Technical Program Chairman for the 1988 IEEE Antennas and Propagation Society International Symposium and URSI Radio Science Meeting. He has been appointed U.S. Research Council Representative to many URSI General Assemblies. He is the Chairman of the Intercommission Working Group of International URSI on Time Domain Metrology. Dr. Sarkar is a member of Sigma Xi and the International Union of Radio Science Commissions A and B. He is a Fellow of the IEEE.

FENGDUO HU was born in China in 1963. He received the B.S. degree in electrical engineering from Southeast University, Nanjing, China, in 1985, and the M.S. and Ph.D. degrees in electrical engineering from Syracuse University, Syracuse, NY, in 1988 and 1990, respectively. From 1986 to 1990 he was a research assistant in the Department of Electrical Engineering, Syracuse University, where he worked on the development and analysis signal processing algorithms for electromagnetic systems. During 1991–1992 he was a research scientist at Entropic Speech, Inc., Cupertino, California. He worked on the research and development of low bit rate speed coders and echo cancelers. Since 1993 he has been with Zilog, Inc., Campbell, California, where he currently works on system designs for consumer electronics products. His research interests are in the areas of spectrum estimation, speech synthesis, speech coding, system theory and fast algorithms.

YINGBO HUA was born in Wu-Xi, Jiangsu, China, on November 26, 1960. He received the B.S. degree in control engineering from Southeast University (Nanjing Institute of Technology), Nanjing, Jiangsu, China, in 1982, and the M.S. and Ph.D. degrees in electrical engineering from Syracuse University, Syracuse, NY, in 1983 and 1988, respectively. He was a graduate teaching assistant from 1984 to 1985, a university graduate fellow from 1985 to 1986, a graduate research assistant from 1986 to 1988, and a postdoctoral research associate from 1988 to 1989, all at Syracuse University. Since 1990, he has been with the University of Melbourne, Victoria, Australia, where he is now a senior lecturer. He has published over 50 articles. His current interests include spectral estimation, array processing, and radar imaging. He is a Senior Member of IEEE.

MICHAEL WICKS received his BSEE degree from Rensselaer Polytechnic Institute, Troy, NY, in 1981, and his MSEE degree from Syracuse University in 1985. He has been with the Rome Laboratory at Griffiss AFB, NY, since 1981, where he works in the Signal Processing Branch of the Directorate of Surveillance and Photonics. He is active in the areas of detection and estimation theory, radar clutter measurements and analysis, wideband radar technology, bistatic and polarimetric radar applications, and modern signal processing techniques. He is the author of many technical reports, articles, and patent applications.